Erschienen in: Energy Procedia ; 55 (2014). - S. 295-301

Available online at www.sciencedirect.com

ScienceDirect

Energy Procedia 55 (2014) 295 – 301

Energy Procedia

4th International Conference on Silicon Photovoltaics, SiliconPV 2014

# Etch-back of $p^+$ structures for selective boron emitters in n-type c-Si solar cells

Yvonne Schiele*, Sebastian Joos, Giso Hahn, Barbara Terheiden

*University of Konstanz, Department of Physics, P.O. Box 676, D-78457 Konstanz, Germany*

**Abstract**

In order to minimize electrical losses in the phosphorous emitter being one of the dominant factors limiting the performance of standard screen-printed p-type c-Si solar cells, selective emitter structures have been introduced to advanced standard p-type solar cells in recent years. A selective emitter is expected to yield various benefits for many different kinds of n-type solar cell concepts as well. The technical implementation of such a selective $p^+$ diffused Si region by wet chemical etch-back of the heavily doped Si wafer surface via porous Si (por-Si) formation is developed into a well controllable process using a new etching solution adapted for $p^+$ doped Si layers in respect of their higher concentration of valence band holes. As an initial proof of concept, integrated into 100 µm thin n-type bifacial large-area Si solar cells, the selectively etched-back B emitter yields a $V_{OC}$ gain of 5 mV and an $R_{shunt}$ increase by a factor of 20.

© 2014 The Authors. Published by Elsevier Ltd. This is an open access article under the CC BY-NC-ND license (http://creativecommons.org/licenses/by-nc-nd/3.0/).
Peer-review under responsibility of the scientific committee of the SiliconPV 2014 conference

*Keywords:* n-type; selective; boron; emitter etch-back

## 1. Introduction

Electrical losses in the phosphorous emitter as one of the dominant factors limiting the performance of standard screen-printed p-type c-Si solar cells gave reason to develop selective emitter structures for advanced standard p-type solar cells in recent years. A technical implementation of such a selective $n^+$ region is the wet chemical etch-back of the heavily doped Si wafer surface via porous Si formation and subsequent removal of the porous layer

* Corresponding author. Tel.: +49-7531-88-4995; fax: +49-7531-88-3895.
*E-mail address:* yvonne.schiele@uni-konstanz.de

*Konstanzer Online-Publikations-System (KOPS)*
*URL: http://nbn-resolving.de/urn:nbn:de:bsz:352-0-281468*

1876-6102 © 2014 The Authors. Published by Elsevier Ltd. This is an open access article under the CC BY-NC-ND license (http://creativecommons.org/licenses/by-nc-nd/3.0/).
Peer-review under responsibility of the scientific committee of the SiliconPV 2014 conference
doi:10.1016/j.egypro.2014.08.086

which was introduced by Haverkamp et al. [1] based on an approach of Zerga et al. [2]. This approach permits fine controlling of por-Si layer thickness, i.e. target sheet resistance $R_{sh}$. Furthermore, solely a single diffusion process is required and the additional processes can completely be carried out by industrial processing equipment.

Solar cells based on n-type doped c-Si wafers have raised growing interest in the recent past (e.g. [3-6]) since they feature obvious advantages over standard p-type Si substrate material: a higher tolerance of some residual metal impurities generally allowing higher carrier diffusion lengths [7], and the nonoccurrence of boron-oxygen complex related light-induced degradation (LID) of solar cell performance [8].

A selective $p^+$ emitter is expected to yield additional benefits for many different kinds of n-type solar cell concepts:

- The trade-off between high surface doping concentration to achieve low contact resistance to the screen-printed Ag/Al metalization on the one hand and high emitter $R_{sh}$ to minimize emitter saturation current density $j_{0e}$ on the other hand necessary with homogeneous emitters can be avoided.
- In order to induce better shielding of the highly recombinative metal contacts and to avoid shunting of the p-n junction, deeper $p^+$ emitter profiles can be employed beneath the metal contacts. The latter applies especially to co-fired Ag/Al paste as it is used for contacting boron doped Si because of Al spiking into the emitter [9].
- Employing a deeper B profile beneath the metal contacts may additionally yield a lower contact resistivity [10]. Fritz et al. [11], too, have found that emitter properties other than surface doping concentration influence the quality of the contact to a boron diffused Si region while for $POCl_3$ diffused layers, mainly a very high P concentration at the surface is essential [12].
- Due to the higher solubility of B in $SiO_x$, grown during the diffusion process, than in Si, the $BBr_3$ diffused profile typically exhibits a [B] depletion towards the wafer surface [13] which is identified to cause excessive surface recombination [14]. This can be eliminated by removing the depleted layer by means of boron emitter etch-back (B-EEB). For this purpose, B-EEB is required also in the metal contact area.
- Despite a post-oxidation step during the $BBr_3$ diffusion process, the borosilicate glass (BSG) layer tends to be hard to remove in HF solution. B-EEB as part of the solar cell process may reliably etch off the BSG due to $HNO_3$ added to HF. A completely removed BSG allows better passivation of the $p^+$ Si layer beneath.

## 2. Developing the boron emitter etch-back process

An appropriate wet chemical solution for boron emitter etch-back is required to have certain properties. In particular, the etching needs to be homogeneous on a large-area Si wafer and the etching rate of the solution, thus the target thickness of the removed Si layer (i.e. target $p^+$ $R_{sh}$) has to be controllable and adjustable along with maintaining reasonable process durations. Good controllability is achieved by etching the $p^+$ region via formation of a por-Si layer which is subsequently removed.

An acidic solution composed of HF, $HNO_3$ and $H_2O$ (stain etching) provides higher etching homogeneity and better process control than its alkaline counterpart [1] because stain etching is – due to its electrochemical nature (involving electron transfer as part of the surface reactions) – a self-limiting process, thus can form por-Si in contrast to hydroxide based solutions [15,16].

For EEB in a stain etching solution, the underlying redox reaction is

$$3\mathrm{Si} + 4\mathrm{HNO_3} + 18\mathrm{HF} \rightarrow 3\mathrm{H_2SiF_6} + 4\mathrm{NO} + 8\mathrm{H_2O} + 3(4-m)\mathrm{h^+} + 3(4-m)\mathrm{e^-}\ . \quad (1)$$

Points on the Si surface randomly become oxidation or reduction sites acting as localized electrochemical cells and sustaining currents on the surface. The oxidation on an anodic site consists in

$$\mathrm{Si^0} + 2\mathrm{H_2O} + m\,\mathrm{h^+} \rightarrow \mathrm{SiO_2} + 4\mathrm{H^+} + (4-m)\mathrm{e^-} \quad (2)$$

while the reduction on a cathodic site is

$$HNO_3 + 3H^+ \rightarrow NO + 2H_2O + 3h^+ \cdot \quad (3)$$

In contrast to a polishing stain etch, for por-Si formation, some sites are more frequently anodic than they are cathodic. Once an etch pit is formed, quantum confinement leads to a shielding of the pore walls and etching proceeds only at the pore bottom towards the Si bulk.

Por-Si formation is initiated by valence band holes on the Si surface (cf. (2)) being products of the reduction (3). Thus, the injection of $h^+$ into the valence band is the crucial role of the oxidant and its electrochemical potential is a control parameter to influence por-Si formation. $HNO_3$-rich stain etch solutions induce electropolishing, whereas in HF-rich solutions, the process is limited by the availability of holes, thus por-Si is formed [15].

The density of free valence band holes in $p^+$ layers is higher compared to $n^+$ layers. Thus, for stain etching B doped regions, the $HNO_3$ content in the B-EEB solution required to form por-Si is lower. Moreover, $HNO_3$ content has to be reduced to avoid electropolishing.

Employing the same stain etching solution as for EEB of $n^+$ Si yields very nonuniform B doped layers with unreasonably high $R_{sh}$ values. Using an adapted etching solution with modified concentrations of the chemicals, the BSG is removed reliably and faster whereupon the B diffused layer is etched-back homogeneously and in a controllable manner. As an example, Fig. 1 (left) depicts the depth profiles of a 20 and 50 Ω/sq B doped layer (blue) which are etched-back to ~100 Ω/sq (red) by means of the developed B-EEB solution. A SEM micrograph of the etched-back 20 Ω/sq layer (Fig. 2 right) demonstrates the por-Si formation during B-EEB process. The measured por-Si thickness correlates with the depth difference of the etched-back ECV profile being shifted by ~470 nm to attain congruence with the starting profile (cf. Fig. 1 left).

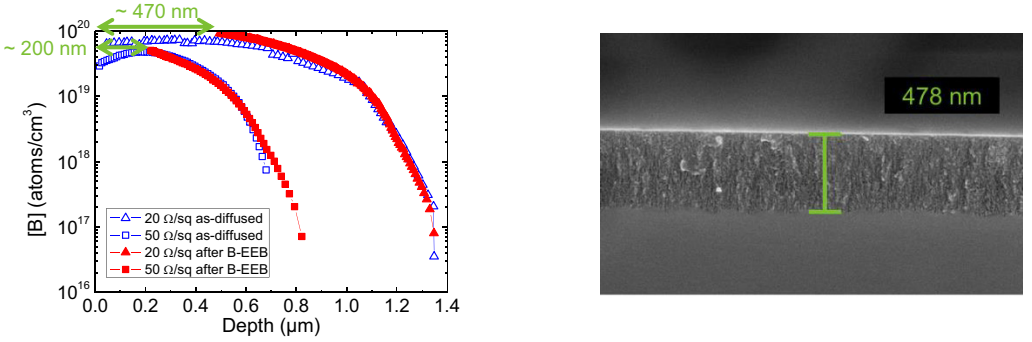


Fig. 1. Left: B concentration profile of a 20 and 50 Ω/sq $p^+$ region after $BBr_3$ diffusion and after subsequent B-EEB to 100 Ω/sq determined by ECV. Right: Cross sectional SEM micrograph of the 20 Ω/sq $BBr_3$ diffused Si wafer surface etched-back to 100 Ω/sq by creating a ~470 nm thick por-Si layer.

A 30 Ω/sq $BBr_3$ diffused layer on a large-area alkaline textured Cz-Si substrate is subjected to B-EEB for various etching durations yielding $R_{sh}$ of up to 120 Ω/sq within 12 min (Fig. 2). $R_{sh}$ initially increases hardly due to remaining BSG on the surface and due to the relatively constant or depleted doping concentration and the absence of the kink/tail shape. The increase of the etching rate with layer depth is then caused by the more pronounced decline of [B]. $R_{sh}$ variation on the large-area wafer (error bars in Fig. 2) increases with etching duration indicating a [B] dependent etching rate. In general, the etching rate can easily be modified by changing the $H_2O$ dilution rate of the B-EEB solution.

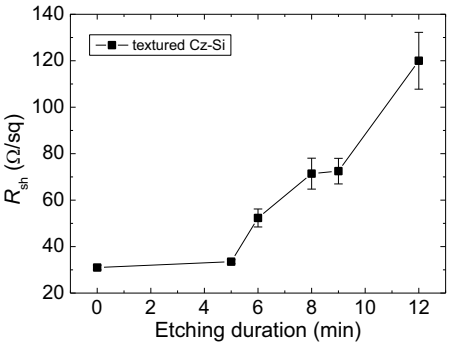


Fig. 2. $R_{sh}$ of a 30 Ω/sq B doped layer (as-diffused) on a textured Cz-Si surface versus B-EEB duration. The error bars result from the variation of $R_{sh}$ determined in different locations on the 125×125 mm$^2$ wafer by four-point probe method.

For the insertion of a selective B emitter into an n-type solar cell process, a 30 Ω/sq $BBr_3$ diffused starting emitter is subjected to B-EEB for different etching periods yielding $R_{sh}$ between 70 and 130 Ω/sq which result from different profile depths and surface doping concentrations (Fig. 3 left). The corresponding ECV profiles are measured after the complete solar cell process which means that high temperature steps followed the B-EEB process and modified the profile shape again (cf. Fig. 4).

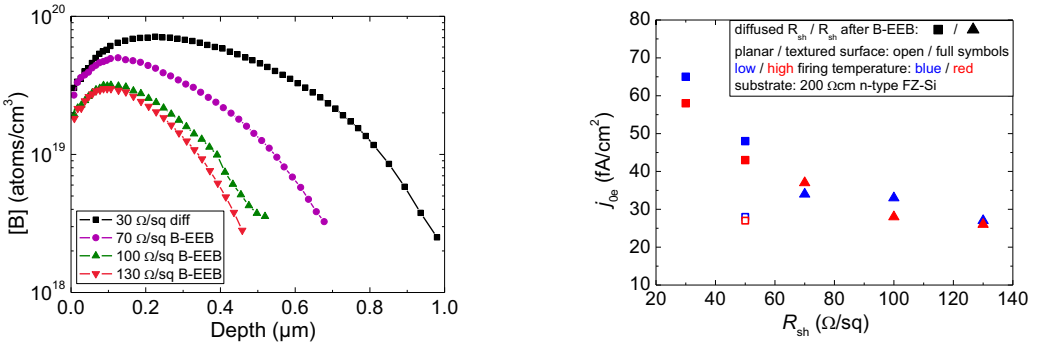


Fig. 3. Left: Profiles of 30 Ω/sq B emitter successively etched-back to different $R_{sh}$ determined by ECV after subjecting to solar cell process (cf. sec. 3). Particularly the thermal oxidation (900°C for a few minutes) creating the passivation layer causes another B depletion at the wafer surface. Right: $j_{0e}$ of B emitters with different $R_{sh}$ (as-diffused) and of the 30 Ω/sq emitter etched-back to different $R_{sh}$ (passivation like in solar cell process, substrate 200 Ωcm n-type FZ-Si).

The corresponding $j_{0e}$ of the profiles in Fig. 3 (left) are depicted in Fig. 3 (right) together with further non-etched-back B emitters featuring $R_{sh}$ between 30 and 130 Ω/sq. Independent of B-EEB employment, $j_{0e}$ diminishes with increasing $R_{sh}$. On planar wafer surfaces, generally lower $j_{0e}$ than on alkaline textured surfaces are achieved. A peak firing temperature difference of 70 K has no significant influence on $j_{0e}$.

## 3. N-type solar cells with selectively doped structures

As an initial proof of concept in solar cells, the novel B-EEB (green in Fig. 4) together with the corresponding process for phosphorus doped layers (red in Fig. 4) is inserted into an n-type bifacial solar cell processing sequence as optional improvements in order to create either a selectively etched-back $p^+$ emitter or a selective $n^+$ back surface field (BSF). Both sides of the solar cell are textured. Boron emitter and phosphorous BSF are passivated by stacks of dielectric layers. The metal finger grids are all screen-printed (Fig. 4).

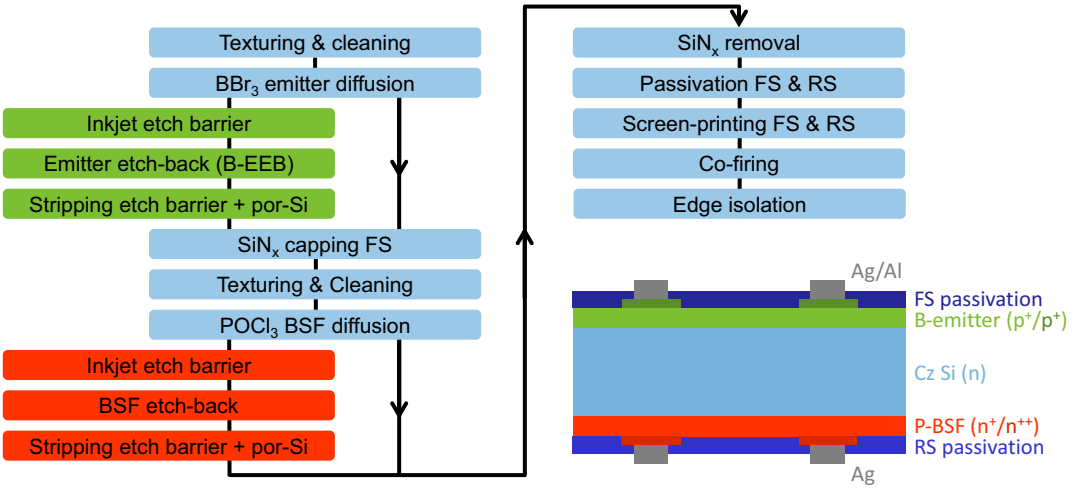


Fig. 4. Processing sequence for screen-printed bifacial n-type solar cells with optional steps for selective $p^+$ emitter and selective $n^+$ BSF; schematic representation of the final solar cell featuring selective doping structures on both sides.

100 µm thin bifacial solar cells with selectively doped structures on both sides created by applying the additional process steps are compared with homogeneously doped devices (Tab. 1). In both approaches, advanced $BBr_3$ diffused starting $p^+$ layers (homogeneous: $R_{sh} = 50$ Ω/sq, selective: $R_{sh} = 30$ Ω/sq + B-EEB) are employed [17]. At the rear, a homogeneous 60 Ω/sq $n^+$ BSF is compared with a $POCl_3$ diffusion of $R_{sh} = 40$ Ω/sq + EEB.

In order to structure the selective $p^+$ and $n^+$ layers, an inkjet-printed shadow mask shields the areas beneath the metal contacts from being etched [18]. After EEB, the mask is removed together with the por-Si in KOH solution.

IV measurement of the bifacial solar cells is carried out using a non-reflective and non-conductive IV chuck. A reflective but non-conductive chuck increases short circuit current density $j_{SC}$ by ~ 0.6 mA/cm$^2$ yielding a maximum efficiency $\eta$ of 19.8% (bifaciality = 99.6%).

Table 1. IV characteristics of the manufactured bifacial solar cell types (5 inch n-type Cz-Si, thickness = 100 µm, $\rho_{base} = 2.0$-$4.5$ Ωcm, $\tau_{base} \approx 7$ ms) measured using a black chuck.

| Solar cell type | $V_{oc}$ (mV) | $j_{sc}$ (mA/cm$^2$) | *FF* (%) | $\eta$ (%) | $R_{ser}$ (Ωcm$^2$) | $R_{shunt}$ (kΩcm$^2$) | *Bifaciality* (%) |
|---|---|---|---|---|---|---|---|
| Hom. $p^+$ emitter, hom. $n^+$ BSF | 644 | 37.1 | 78.3 | 18.7 | 0.46 | 3.6 | 94.3 |
| Sel. $p^+$ emitter, hom. $n^+$ BSF | 649 | 37.0 | 77.3 | 18.5 | 0.58 | 72.8 | 95.9 |
| Sel. $n^+$ BSF, hom. $p^+$ emitter | 661 | 37.6 | 78.4 | 19.5 | 0.46 | 67.6 | 99.4 |

The increased open circuit voltage $V_{OC}$ of the selectively doped solar cells (Tab. 1) reflects the reduced $j_{0e}$ in the etched-back regions (cf. Fig. 3, right). Beneath the metal contacts, the deeper doping profiles induce better shielding of the highly recombinative contacts.

Due to the "kink and tail" shape of a $POCl_3$ diffused profile, the $V_{OC}$ gain by a selective $n^+$ BSF is very high (17 mV) combined with a $j_{SC}$ increase of 0.5 mA/cm$^2$. In the passivated $n^+$ areas, $j_{0BSF}$ is reduced by EEB from ~200 fA/cm$^2$ (40 Ω/sq) to ~30 fA/cm$^2$ compared to ~130 fA/cm$^2$ (60 Ω/sq) in the homogeneous case. By employing the selectively etched-back B emitter, a $V_{OC}$ gain of 5 mV is achieved along with maintaining $j_{SC}$ (reduction of $j_{0e}$ by B-EEB from ~60 fA/cm$^2$ to ~30 fA/cm$^2$ in the passivated $p^+$ areas vs. 45 fA/cm$^2$ in the homogeneous case, cf. Fig. 3). The relatively poor $j_{SC}$ can easily be enhanced by thickening the wafer (from 100 µm to 175 µm: $\Delta j_{SC} \approx 0.5$ mA/cm$^2$) or reducing finger width (from 110 µm to 70 µm: $\Delta j_{SC} \approx 1.1$ mA/cm$^2$). An additional $V_{OC}$ and $j_{SC}$ gain may be attained by inserting the B-EEB into the solar cell processing sequence not before, but after the high temperature $POCl_3$ diffusion and thermal oxidation [10]. In this case, the [B] depletion at the wafer surface would be removed and surface recombination may be reduced.

Because of a diminished fill factor *FF* and a risen series resistance $R_{ser}$ (Tab. 1), the selective $p^+$ emitter solar cell does not exploit its full potential. This is caused by the smaller lateral conductivity of the higher $R_{sh}$ emitter between the metal contacts and prevents $j_{SC}$ from being enhanced compared to the homogeneous emitter solar cell. Contact resistivity, however, is not supposed to be an issue as depth and surface doping concentration of the selective $p^+$ emitter beneath the contacts are higher than in the homogeneous case (cf. Fig. 3, left).

$R_{shunt}$ is considerably enhanced (by a factor of ~20) by implementing a selective $p^+$ or $n^+$ structure. In the case of the selective $p^+$ layer, the deeper emitter profile beneath the metal contacts reduces the shunting of the p-n junction. In the case of the selective $n^+$ layer, the emitter profile is also deeper compared to the homogeneous solar cell, but caused by the higher temperatures during the heavier $POCl_3$ diffusion.

All solar cell types exhibit very high bifaciality = $\eta_{RS}/\eta_{FS}$ of >94% which is further increased by the selective $p^+$ or $n^+$ layer. The selective $n^+$ layer yields bifaciality of >99% because $\eta_{RS}$ is enhanced due to a significantly reduced recombination at the front.

## 4. Conclusion and outlook

The technical implementation of a selective $p^+$ region by wet chemical etch-back of the heavily doped Si wafer surface via porous Si formation has been developed into a well controllable process using a new etching solution adapted for $p^+$ doped Si layers in respect of their higher concentration of valence band holes.

Integrated into initial 100 µm thin n-type bifacial large-area solar cells as a proof of concept, the selectively etched-back B emitter has yielded a $V_{OC}$ gain of 5 mV and an $R_{shunt}$ increase by a factor of 20. Using a selective phosphorous BSF in the solar cell created by the equivalent process for $n^+$ layers, conversion efficiency of up to 19.5% with $V_{OC}$ = 661 mV and bifaciality of 99.4% have been achieved on a black and non-conductive measuring chuck.

Further optimized solar cells featuring a combination of selective structures on both sides and an etched-back $p^+$ emitter without surface [B] depletion are anticipated to attain efficiencies of >20%.

## Acknowledgements

The research leading to these results has received funding from the European Union Seventh Framework Programme (FP7/2007-2013) for the Collaborative Project (CP) '20plµs' with the full title: ‘Further development of very thin wafer based c-Si photovoltaics' under grant agreement n° 256695. Part of this work was supported by the German Federal Ministry for the Environment, Nature Conservation and Nuclear Safety. The content of this publication is the responsibility of the authors.

## References

[1] Haverkamp H, Dastgheib-Shirazi A, Raabe B, Book F, Hahn G. Minimizing the electrical losses on the front side: Development of a selective emitter process from a single diffusion. In: Proc 33rd IEEE PVSC. San Diego, CA, USA; 2008. p. 430-3.

[2] Zerga A, Slaoui A, Muller JC, Bazer-Bachi B, Ballutaud D, Le Quang N, Goaer G. Selective emitter formation for large-scale industrially mc-Si solar cells by hydrogen plasma and wet etching. In: Proc 21st EU PVSEC. Dresden, Germany; 2006. p. 865-9.

[3] Zhao J, Wang A, Altermatt PP, Green MA, Rakotoniaina JP, Breitenstein O. High efficiency PERT cells on n-type silicon substrates. In: Proc 29th IEEE PVSC. New Orleans, LA, USA; 2002. p. 218-21.

[4] Kiefer F, Ulzhöfer C, Brendemühl T, Harder NP, Brendel R, Mertens V, Bordihn S, Peters C, Müller JW. High efficiency n-type emitter-wrap-through silicon solar cells. IEEE J Photov 2011;1(1):49-53.

[5] Benick J, Hoex B, van de Sanden MCM, Kessels WMM, Schultz O, Glunz SW. High efficiency n-type Si solar cells on $Al_2O_3$-passivated boron emitters. Appl Phys Lett 2008;92:253504.

[6] Schiele Y, Book F, Seren S, Hahn G, Terheiden B. Screen-printed Al-alloyed rear junction solar cell concept applied to very thin (100 µm) large-area n-type Si wafers. En Proc 2012;27:460-6.

[7] Macdonald D, Geerligs LJ. Recombination activity of interstitial iron and other transition metal point defects in p- and n-type crystalline silicon. Appl Phys Lett 2004;85:4061-3.

[8] Glunz SW, Rein S, Lee JY, Warta W. Minority carrier lifetime degradation in boron-doped Czochralski silicon. J Appl Phys 2001;90:2397-404.
[9] Lago R, Pérez L, Kerp H, Freire I, Hoces I, Azkona N, Recart F, Jimeno JC. Screen printing metallization of boron emitters. Prog Photovoltaics: Res Appl 2010;18:20-7.
[10] Schiele Y, Hahn G, Terheiden B. Contacting and recombination analysis of boron emitters via etch-back for advanced n-type Si solar cells. 29th EU PVSEC. Amsterdam, The Netherlands; 2014; accepted.
[11] Fritz S, Riegel S, Gloger S, Kohler D, König M, Hörteis M, Hahn G. Influence of emitter properties on contact formation to $p^+$ silicon. En Proc 2013;38:720-4.
[12] Schubert G. Thick film metallization of crystalline silicon solar cells: mechanisms, models and applications. PhD thesis, University of Konstanz; 2006.
[13] Masetti G, Solmi S, Soncini G. Boron redistribution at oxide-silicon interface during drive in in oxidizing atmospheres. Electron Lett 1973;9:226-8.
[14] Li X, Tao L, Xia Z, Yang Z, Dong J, Song W, Zhang B, Sidhu R, Xing G. Boron diffused emitter etch back and passivation. In: Proc 37th IEEE PVSC. Austin, TX, USA; 2012. p. 1073-6.
[15] Kolasinski KW. Silicon nanostructures from electroless electrochemical etching. Curr Opin Solid St M 2005;9:73-83.
[16] Kolasinski KW. Growth and etching of semiconductors. In: Hasselbrink E, Lundqvist I, editors. Handbook of surface science. Vol. 3, Amsterdam: Elsevier; 2008. p. 787-870.
[17] Schiele Y, Fahr S, Joos S, Hahn G, Terheiden B. Study on boron emitter formation by $BBr_3$ diffusion for n-type Si solar cell applications. In: Proc 28th EU PVSEC. Paris, France; 2013. p. 1242-7.
[18] Lauermann T, Dastgheib-Shirazi A, Book F, Raabe B, Hahn G, Haverkamp H, Habermann D, Demberger C, Schmid C. INSECT: An inline selective emitter concept with high efficiencies at competitive process costs improved with inkjet masking technology. In: Proc 24th EU PVSEC. Hamburg, Germany; 2009. p. 1767-70.